An Experimental Investigation of the Electrodeless Traveling Wave Accelerator for Wind-Tunnel Application

G. R. SEEMANN*
McDonnell Douglas Astronautics Company—Western Division, Santa Monica, Calif.

AND

J. A. THORNTON† AND A. S. PENFOLD‡
Telic Corporation, Santa Monica, Calif.

This paper describes an experimental investigation conducted to examine some of the physical processes that determine the density range over which traveling wave accelerators can be operated effectively. The experiments were conducted with two constant-field-velocity, constant-channel-diameter accelerators, using argon as the principal test gas. One accelerator was operated primarily subsonically, while the second accelerator was operated supersonically. Power inputs with the subsonic accelerator were in the range 50 to 100 kw with exit velocities of about 1000 m/sec. Gas densities were in the range 9×10^{-6} kg/m^3 to 8×10^{-4} kg/m^3. The experiments indicate that the energy exchange within the accelerator channel was controlled to a significant extent by Coulomb collisions and that the electron-energy distribution may have been non-Maxwellian. Power inputs with the supersonic accelerator were in the range 250 w to 2.5 kw. Exit velocities were in the range 2000–2700 m/sec with Mach numbers in the range of 1.5–2.2. Gas densities ranged from 10^{-4} kg/m^3 to 5×10^{-4} kg/m^3. Although evidence of considerable end-field joule heating was observed, the experiments were in general agreement with one-dimensional fluid dynamic theory and indicate promise for the application of traveling wave accelerators to wind tunnels in the altitude range of 150,000–300,000 ft.

Introduction

THE electrodeless traveling wave accelerator uses the process of magnetic induction to avoid the well-documented electrode problems[1] that have characterized much of the Faraday and Hall current accelerator work. Thus, it is desirable to apply the traveling wave concept for accelerating gas streams of sufficient density to be useful for wind-tunnel applications. Unfortunately, most of the published experimental work pertaining to traveling wave accelerators has dealt with the acceleration of low-density (less than 10^{-6} kg/m^3) gas streams for propulsion applications.[2,3] This paper describes the results of an experimental study[4,5] that was performed to investigate some of the physical processes which are encountered at higher densities and which determine the feasibility of using the traveling wave accelerator to accelerate gas streams of sufficient density so as to be useful for wind-tunnel applications.

Design and Scaling Laws

In their most general configurations both the traveling wave and the Faraday devices produce the desired acceleration in a confined channel by the interaction of an externally applied magnetic field with orthogonal currents which are made to flow in a gas that is electrically conducting because it is partially ionized. Thus, in the limit of one-dimensional flow, both devices are governed by identical forms of the equations of MHD—the only difference being that, in the case of the traveling wave accelerator,[6] the electron drift velocity ($V_D = E/B$, where E is the electric field strength and B is the magnetic field strength) is recognized as being equal to the magnetic field velocity V_f. Thus, the same first-order design analysis is applicable to both classes of devices.

Resler and Sears[7] have investigated the quasi-one-dimensional MHD equations for the acceleration of a perfect gas with a constant electrical conductivity in a constant area channel having a distribution of magnetic and electric fields that gave a constant drift (field) velocity. They have presented their results in a phase plane (Fig. 1) which clearly shows the design constraints that are introduced by the confining channel. The ordinate u/V_f, where u is the gas velocity, is equivalent to the ratio of the rate at which work is done on the gas stream by the Lorentz force to the rate of energy addition by joule heating. In Fig. 1, the line located at $u/V_f = (\gamma - 1)/\gamma$, where γ is the ratio of specific heats, is called the "thermal limit." Along the thermal limit the Lorentz force is balanced by the pressure gradient that results from the joule heating. Below, the thermal limit pressure gradients (due to joule heating) are dominant, while above the thermal limit the Lorentz force is dominant in determining the spatial change in the flow velocity. There is considerable doubt about the stability of the solution that passes through Mach 1 (Ref. 8). Thus a re-entry simulator must be designed to operate in Quadrant IV.

First-order design and scaling laws can be formulated by combining the one-dimensional fluid dynamic conservation equations with the auxiliary equations of state, electrodynamics, heat transfer, and friction. When this is done it is found that the number of parameters introduced is greater than the number of equations. Thus, one is free to impose additional conditions or equations. Ring,[9] has considered the design analysis as a problem in the calculus of variations, investigating those additional operating conditions that would permit the accelerator to have a maximum energy input with a minimum length. Ring found that the magnetic field

Received July 11, 1969; revision received December 15, 1969. This investigation was performed under the sponsorship of the Air Force Flight Dynamics Laboratory, Wright-Patterson Air Force Base, Ohio, under Contract AF33(612)-2548 while the authors were associated with the Space Sciences Laboratories, Litton Systems Inc., Beverly Hills, Calif.

* Section Chief, Thermal-Optics Research and Development. Associate Fellow AIAA.

† Director, Research and Development. Associate Fellow AIAA.

‡ Vice President. Associate Fellow AIAA.

could not be optimized since a minimum length leads to an infinite field. A similar situation arose when an optimum gas temperature was sought. The optimization analysis indicated that the accelerator should operate at near-sonic conditions in the accelerator section. Obviously, this cannot be done since to achieve the ultra-high velocities of interest; the temperature would be too high to maintain the integrity of the channel walls. Therefore, two useful design considerations for the general MHD-channel-type wind-tunnel accelerator are; 1) the magnetic field strength should be constant along the channel at the maximum practical value, and 2) the channel cross section should be varied so as to maintain the gas temperature essentially constant at a value that is high enough to assure a significant electrical conductivity and low enough to minimize the degree of dissociation and damage to the channel walls. At this point two important practical differences between the traveling wave and Faraday accelerators are recognized; i.e., the traveling wave devices have 1) the advantage that they avoid the use of electrodes, and 2) the disadvantage that their operating regimes are limited by the limited magnetic field strengths that can be produced.

In the case of the Faraday accelerator, magnetic field strengths up to 3 webers/m^2 have been used and 10 webers/m^2 are projected.[10] Thus, considerable freedom is available in specifying the channel shape and length. This permits a channel design that minimizes heat transfer and friction and incorporates an exit-expansion nozzle for increasing the Mach number.

In the case of the traveling wave accelerator, the radial (accelerating) components of the traveling magnetic field will probably be limited to values of less than 0.3 weber/m^2 (Ref. 11). This reduced magnetic field strength dictates that the traveling wave accelerator be designed to have a channel that is, in general, considerably longer than those used for comparable Faraday accelerators and that careful attention be given to the effects of heat transfer and friction.

First-order traveling wave accelerator design calculations were made by combining the one-dimensional conservation equations with the perfect gas equations of state and Ohm's law, and by using Reynold's analogy (assuming turbulent flow). The magnetic field strength, gas temperature, and electrical conductivity were assumed constant along the channel. Figure 2 shows typical results of numerical solutions of these equations. In making the calculations the field velocity was varied along the accelerator channel in such a way as to control the joule heating and thereby to limit the channel area change (e.g., the decrease in gas density) that was required to maintain the gas temperature constant. The altitude, density, and velocity conditions in the test section for various magnetic field strengths are shown in Fig. 3. The projected performance shown in Fig. 3 is considerably better than that which was indicated in preliminary estimates.§

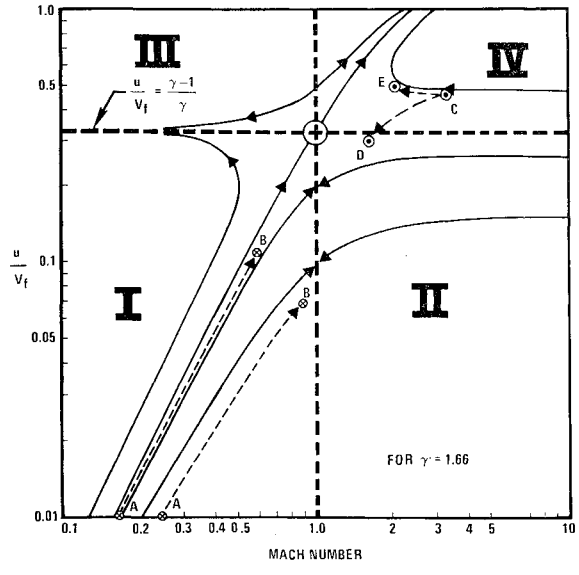

Fig. 1 Electromagnetic acceleration of one-dimensional flow in constant area channel.

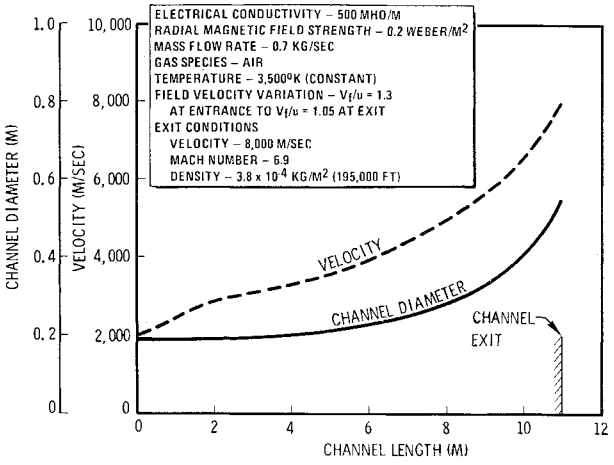

Fig. 2 Numerical computational results for channel flow.

Basis for Experimental Investigation

The results in Fig. 3 are encouraging. However, the assumptions upon which the first-order analysis is based raise questions which require additional investigation. For example; 1) to what degree does the energy-addition process in the traveling wave accelerator depart from the approximation provided by the one-dimensional equations (e.g., effects such as those induced by the fringe fields at the entrance and exit of the channel), and 2) what is the particular nature of the ionization production-and-loss mechanisms that result from the azimuthally symmetric electrodeless discharge and determine the plasma conductivity in the accelerator?

The experimental research concentrated on certain aspects of these questions. In order to simplify the interpretation of the experimental results and to permit a correlation with the considerations summarized in Fig. 1, the experiments were

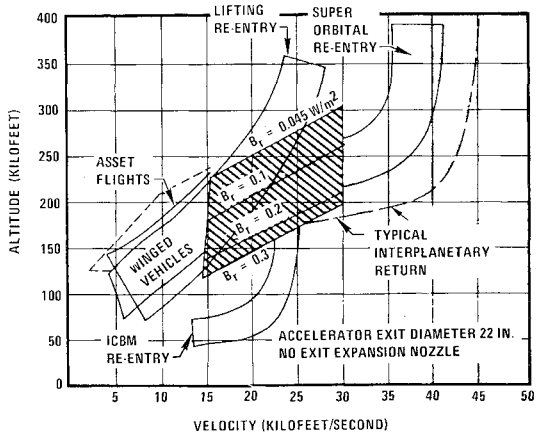

Fig. 3 Required magnetic field strengths for projected velocity-altitude range.

§ Using a simple magnetic piston model and comparable values of the magnetic field strength, Ring[10] estimated that the region of applicability of the traveling wave accelerator would be limited to the altitude range 280,000 to 400,000 ft.

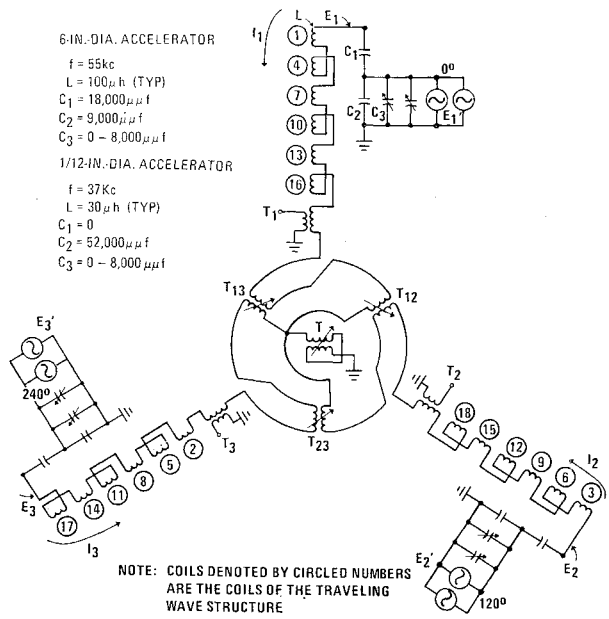

Fig. 4 Accelerator electrical circuit schematic.

conducted with a constant field velocity in channels with constant cross sections.

As a general rule the relative performance of electrodeless induction devices improves as they become larger. This is seen by the size of the accelerator referred to in Fig. 2 and is a consequence of the relatively weak magnetic fields and the effects of friction and heat transfer. In order to achieve the desired experimental objectives with available laboratory equipment it was found desirable to assemble two accelerators; 1) a relatively large (6-in.-diam channel) accelerator with a high field velocity (20,600 m/sec),[12] and 2) a smaller ($1\frac{1}{2}$-in.-diam channel) accelerator which had a sufficiently low field velocity (5300 m/sec) so that it could be operated in the IVth quadrant shown in Fig. 1 while using a commercially available plasma jet injector.

The size of the large accelerator permitted instrumentation to be positioned along the accelerator channel. The high field velocity provided relatively large azimuthal electrical fields (~1 v/cm) despite the limited radial magnetic field strengths (B_r = 30–100 gauss) that could be generated with the available power supplies; e.g., $E_\theta = B_r(V_f - u)$. These azimuthal electric field strengths were adequate to cause power transfers to the gas stream (50–100 kw) which were large enough to facilitate an investigation of those ionization production-and-loss mechanisms which occur in the azimuthally symmetric geometry and which are not particularly dependent on the gas velocity per se.

The small accelerator was designed to accelerate a supersonic gas stream and to permit an examination of the applicability of the one-dimensional flow equations and a determination of the extent of the end field effects. The field region at the entrance and exit of the accelerator channel is a region in which variations in both field velocity and magnetic flux amplitude are encountered. This region may be considered as consisting of the coherent superposition of two electromagnetic fields; 1) a fringe field having a field velocity that is considerably greater than the field velocity in the accelerator channel, and 2) a standing wave field having a field velocity that is zero.[5] Referring to Fig. 1, the standing wave will produce a deceleration of the gas because the gas velocity exceeds the field velocity, and the fringe field will produce excessive joule heating since the gas velocity is less than $(\gamma - 1)/\gamma$ times the field velocity. Both fields produce joule heating because of the axial variations in magnetic flux intensity. The end field effects are particularly important in the acceleration of a supersonic gas stream, since the deceleration and joule heating can cause the channel flow to choke.

Experimental Apparatus

Design of the Magnetic-Field Coil System

Three considerations are important in the coil system design; 1) positioning of the coils so that the radial component of the traveling magnetic field is maximum, 2) positioning of coils to yield desired variations in field velocity, and 3) design of the electrical system so that an efficient coupling between the coil system and the rf power supplies is achieved. The objectives of this work required investigation of the first and third considerations.

The basic problem in generating a high magnetic field is to place as many ampere turns as possible, as close as possible, to the channel wall. The radial component can be increased to a considerable degree by placing a ferrite inner body in the accelerator channel and, to some degree, by placing ferrite around the channel. Ferrites were not used in the present investigation since, in the case of the large accelerator, the inner body was used for diagnostic instrumentation, and in the small accelerator an inner body would have caused excessive wall losses. In the absence of ferrites, there is, for each coil diameter, a unique wavelength of the traveling magnetic field pattern which yields a maximum radial component of the magnetic field at a given radial position within the channel.[5] (For example, at a reference radius of 0.7 times the coil radius R_c the optimum wavelength is about 3.7 R_c.) This relationship was used as a general guideline in the design of both the large and small accelerators.

A continuously operating traveling magnetic field can be formed either by making the magnetic field coils part of a transmission line which is driven at one end by an rf power supply and terminated at the other end with the characteristic impedance of the transmission line, or by making the field coils the inductive links of a system of properly phased resonant circuits. For a given rf power supply, larger coil currents can be achieved by the second technique and it is therefore favored for wind-tunnel applications. However, implementation of the resonant circuit technique posed a number of practical problems. In order to achieve maximum power transfer to the plasma, provisions had to be made for adjusting the individual resonant circuits so that they were electrically uncoupled, and for maintaining this adjustment and the condition of circuit resonance in the presence of plasma loading.

The plasma has three major effects on the coil system: 1) the effective resistance of the coils is increased (a consequence of the work being done on the gas); 2) the effective inductance of the coil is decreased (a consequence of current flow in the gas); and 3) the mutual inductance between the coils is decreased (a consequence of current flow in the gas).

Figure 4 shows a circuit that was found to permit the plasma-induced effects to be compensated for rapidly and effectively.¶ This circuit, which was used for both the large and small accelerators, produced a traveling magnetic field in a system of 18 coils by connecting them in three resonant circuits which were phased 120 electrical degrees apart and designed to match the output impedance of available 50-kw class-C power amplifiers. The coils, which are labeled according to their position along the accelerator channel, were wound in such a way that the currents in adjacent coils were 60 electrical degrees apart.

In the absence of plasma the corrective transformers T_{12}, T_{23}, T_{13} were used to adjust the net mutual inductances to equal values. The motor-driven variometer T was then adjusted to reduce the net mutual inductances to zero, or

¶ The fixed capacitance C_1 was used as a voltage divider for the large accelerator to achieve the desired circulating currents.

near-zero values. The variable capacitors were then used to bring the circuits into resonance. The circuit was designed to take advantage of the fact that when an ionized gas is present the mutual inductances between the tank circuits change by approximately the same amount. Thus, in the presence of a plasma, the variometer could be used to readjust the mutual inductances to a minimum. This is the major readjustment which was necessary. The variable capacitors were then used to make a slight adjustment for resonance. It was found that a useful initial setting of the corrective transformers could be achieved by using the preionizer to fill the channel with a weak plasma, and by keeping the coil currents at a sufficiently low value so that, to first order, the traveling magnetic field did not perturb the weak plasma glow.

Description of 6-in.-diam Accelerator

The basic accelerator structure is shown in Fig. 5. A metered gas flow was injected into the accelerator channel through an annular nozzle and was partially ionized by a 210-kc capacitive discharge which was maintained between an outer ring electrode and a center electrode on the inner body by a 12-kw power supply. Static pressure ports in the injector nozzle permitted an estimate of the velocity of the gas as it entered the traveling field region. Additional static pressure ports were located along the inner body. The channel walls and the inner body were cooled with a metered water flow. An oil bath with a metered oil flow surrounded the accelerator coils.

The field coils consisted of 20 turns of 0.405-in.-diam Litz wire (2000 strands/wire) placed in five layers of four turns each (the last three coils were reduced to four layers in order to reduce the strength of the magnetic field in the fringe field region at the exit). The coils were connected electrically as shown in Fig. 4 and driven at 54 kc × six 50-kw power supplies. The 18 coils provided a six-phase system extending over three wavelengths with a field velocity of 20,600 m/sec. At resonance the power supplies were capable of causing coil currents of about 100 amp (rms). These currents yielded peak radial magnetic field components of about 100 gauss near the channel wall.

Table 1 Subsonic accelerator—operating conditions

Entrance conditions	
Flow rates:	0.25–5.0 gm/sec argon 0.25–3.0 gm/sec air-argon mixtures (10–60% air)
Velocity:	46–122 m/sec (150 to 400 fps)
Mach No.:	0.10–0.25
Electrical conductivity:	50–100 mho/m argon
Test section conditions	
Velocity:	305–1220 m/sec (1000–4000 fps)
Mach No.:	0.45–0.95
Effective temperature:	1000°–4500°K
Density:	8.2×10^{-4}–9.2×10^{-1} Kg/m^3
Static pressure:	0.065–3 torr
Miscellaneous data	
Field velocity:	21,600 m/sec
Magnetic field strength, B_r:	30–100 gauss
Total power input:	10–125 kw
Accelerator thermal efficiency:	29–37% (inner body) 45–58% (without inner body)
Axial hall voltage:	8–58 v
Run times:	5–15 min (typical) 90 min (maximum)
Beam size:	6-in.-diam exit 15-in.-diam 10 ft downstream
Exit Chamber Pressure:	0.1–5.0 torr

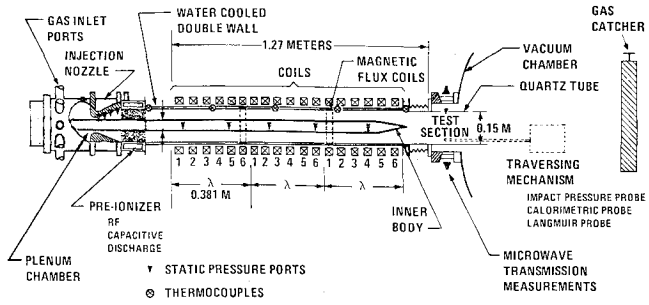

Fig. 5 Subsonic accelerator schematic.

A multi-probe traversing mechanism was used to make detailed measurements of the flow in the test section. Rotation of the traversing mechanism top permitted an impact-pressure probe, a heat-transfer probe, or an electrostatic probe to be positioned in the test section.

Description of the 1½-in.-diam Accelerator

The basic accelerator structure is shown in Fig. 6. A commercial 50-kw plasma jet and supersonic nozzle served as the preionizer injector. The channel walls were cooled by a metered water flow. The field coils consisted of 20 turns of 0.15-in. diam Litz wire placed in five layers of four turns each. The coils were cooled by an oil bath which surrounded them with a metered oil flow. The coils were connected electrically as shown in Fig. 4 and driven at 37 kc × 50-kw power supplies. The maximum coil currents were 80 amp (rms). These currents resulted in peak radial-magnetic field components of about 200 gauss adjacent to the channel walls. Static pressure ports were located at the exit of the supersonic injector and in the test section at the end of the accelerator channel. A series of light pipes was arranged so that the plasma luminosity at several points along the channel could be monitored by photomultipliers.

Experimental Results

Experimental Results with 6-in.-Diam Accelerator

The range of operating conditions for the 6-in.-diam accelerator is listed in Table 1. The channel entrance Mach numbers were estimated from plenum chamber pressures and the pressure variations along the injector nozzle. The entrance electrical conductivities were estimated in preliminary experiments by observing the detuning of an rf coil system placed at the preionizer exit (the rf coil system was calibrated by filling the channel with various conducting solutions).[5,17] The Mach numbers in the test section were calculated from measurements of the impact and static pressures. The gas velocities and densities were estimated from the continuity equation using the measured values for the mass flow and static pressure, and the calculated Mach numbers. The effective temperature is that temperature which is obtained from the perfect gas equation of state, using the measured static pressure and calculated gas density,

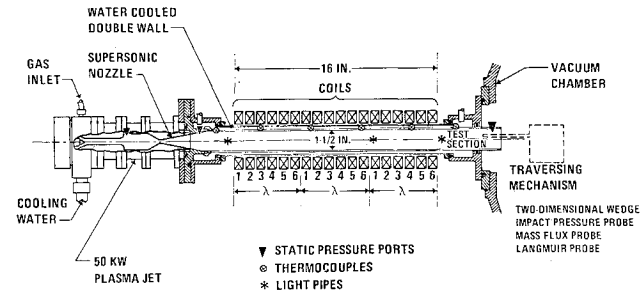

Fig. 6 Supersonic accelerator schematic.

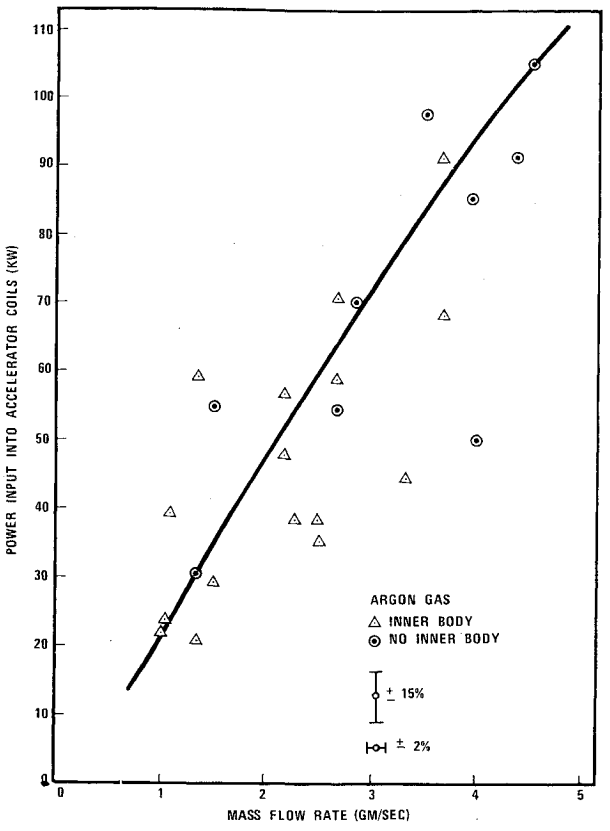

Fig. 7 Power input vs mass flow rate.

i.e., $T_{\text{eff}} = p/\rho R$. (For moderate degrees of ionization the effective temperature will be approximately equal to the gas temperature.) The total power input was determined electrically from the voltage swing across the accelerator coils, the standing plate currents in the power amplifiers (class-C operation), and an empirical constant determined from dummy load experiments. The rf losses in the coil system were determined calorimetrically from the temperature rise of the cooling oil. The power input to the accelerated gas was determined from calorimetric measurements of the power transferred to the accelerator walls (including the inner body), to the traversing mechanism, and to the gas catcher at the accelerator exit. The sum of the powers determined from the monitored coolant flows agreed within 10% of the total power input that was measured electrically.

The experiments showed that electrodeless channel-type accelerators can be operated at relatively high power levels without damage for extended periods of time. During the tests described above, the 6-in.-diam accelerator was operated continuously for as long as 90 min with 70 hr of accumulated test time at power levels in excess of 50 kw with no channel damage whatsoever.

Several observations were made concerning the ionization production-and-loss mechanisms in the acceleration section.

The plasma in the accelerator channel is acted on by two electric fields; the axial field caused by the voltage that is applied to the coil system and the azimuthal field of induction. The axial field had vacuum values of the order of 1000v/cm, while the azimuthal was about 1v/cm. Studies of megacycle rf discharges in unshielded solenoidal discharge tubes in which both the axial and inductive fields are present have identified the existence of two distinct operating modes.[13–15] It has been clearly substantiated that such discharges are ignited into a relatively dim (glow) mode by the axial field and undergo an abrupt transition into an intense bright mode at higher applied potentials due to the inductive field. Recent studies indicate that, at least for pressures greater than about 10^{-1} torr, the bright mode transition voltage at a given pressure is dependent on the electron density in the dim mode plasma.[13]

Two operating modes were observed in the 6-in. accelerator. A dim discharge (power transfer less than 25 w) could be ignited in the accelerator channel when the preionizer was not operated. It is believed that this discharge was ignited by the axial field. At the frequencies used in these experiments the power that could be transferred to the gas by the axial field was very small because the currents had to pass through the nonconducting channel walls as displacement currents. A bright mode transition could not be made to occur without the preionizer in operation, perhaps because the axial field could not transfer enough power to raise the electron density in the accelerator channel up to the critical value necessary for the transition. When the preionizer was operated at near full power (~3 kw) the channel discharge could be made to undergo an abrupt transition into the bright mode.[16]

An interesting observation was made concerning the requirement for azimuthal symmetry in the inductive bright mode discharge. At the high preionizer power levels that were necessary to cause the bright mode transition, particularly at the higher mass flow rates, the capacitive preionizer discharge became asymmetric, developing a series of spoke-like arcs. This asymmetry apparently degraded the performance of the inductive discharge in the accelerator channel; since, once the bright mode transition had been made to occur, additional improvement in the accelerator performance, as manifested by the impact pressure and gas luminosity, could be obtained by reducing the preionizer power level until the spoke arcs (observed through a mirror arrangement) disappeared. Once the bright mode discharge was in operation the preionizer could actually be turned off with only a moderate loss in accelerator performance.

The experimental results permit observations to be made about both the radial and axial variations in the power transfer within the accelerator channel. Power balances for typical test runs, both with and without the inner body installed, are shown in Table 2. A plot of the mass-flow rate versus the input power for the bright mode operation is shown in Fig. 7. It is seen that the input power is essentially independent of the presence or absence of an inner body. Thus, the presence of an inner body simply reduced the energy content of the gas stream (because of heat transfer) while not affecting the power input. This indicates the expected result that most of the power input was adjacent to the outer wall

Table 2 Summary of power transfer measurements[a]

Power transfer	Accelerator channel with inner body	Accelerator channel without inner body
1) Power input to traveling magnetic field	+70 kw	+70 kw
2) Preionizer power input	+2 kw	+1.8 kw
3) Joule losses in magnetic field coils	−10 kw	−10 kw
4) Heat transfer from plasma to inner body	−15.1 kw	−2.9 kw
5) Heat transfer from plasma to channel wall	−24.5 kw	−25.6 kw
6) Heat transfer from plasma to test section wall	−5.5 kw	−7.0 kw
7) Energy flux in plasma passing through test section	(16.9 kw)	(26.3 kw)
8) Heat transfer from plasma to traversing mechanism calorimeter	−12.1 kw	−18.8 kw
9) Heat transfer from plasma to gas catcher	−4.8 kw	−7.5 kw

[a] Based on typical run with argon test gas.

where the radial component of the applied magnetic field was greatest.

The variation in static pressure and heat transfer along the accelerator channel provided an indication of the axial variations in the power input. The Mach number of the gas entering the channel was very low (~0.15). One-dimensional theory predicts that at low Mach numbers the acceleration process should be essentially isobaric but that a slight pressure decrease should occur as the Mach number approaches one. This general type pressure dependence was observed in the experiments. However, the pressure decrease over the last wavelength of the traveling field was rather pronounced indicating that considerable energy addition occurred in the fringe field region near the accelerator exit. This conclusion was supported by the heat-transfer measurements which indicated a higher rate of heat transfer over the last one-third of the machine.

When the power input was plotted as a function of the azimuthal electric field in the channel, it was found that a small increase in the electric field could result in a large increase in the power input, indicating a nonlinear relationship between the plasma electrical conductivity and the azimuthal electric field.[17] If the electrical conductivity of the gas in the accelerator channel, σ, is assumed to be scaler and constant, the total power input to the gas can be approximated by

$$P = J \cdot E(\text{Volume}) = \langle B_r^2 \rangle \sigma V_f (V_f - u) AL \qquad (1)$$

where $\langle B_r^2 \rangle$ is the average value of $\langle B_r^2 \rangle$ across the accelerator channel, A is the channel area, and L is the length of the interaction region. Values of $\langle B_r^2 \rangle$ were estimated by treating the coil system as a stack of current sheets[5] and verified by magnetic-probe measurements in a mock-up coil system. Using these values for the magnetic field strength, and the measured values for the power input P and gas velocity u estimates were made for the average electrical conductivity. For the power input range 10 kw to 125 kw, estimated value of σ varied from 75 to 300 mhos/m in the case where the power transfer was assumed to be uniformly distributed through the channel volume, to 225–900 mho/m when the power transfer was assumed to be concentrated over the last one-third of the machine. In the bright mode of operation the degree of ionization produced by the traveling field was determined by microwave transmission measurements (K and E band) to be about 1% near the accelerator exit. These microwave observations were in general agreement with floating electrostatic-probe measurements at the same position. This relatively high degree of ionization and moderate electrical conductivity suggests that the plasma electrical conductivity may be dominated by Coulomb effects. Since the Coulomb-dominated conductivity of a singly ionized gas is only a function of the electron temperature, the measured conductivities can be used to estimate a value for the electron temperature. At the higher power levels the electron temperatures varied from 3000°K (300 mho/m) to 6000°K (900 mho/m). These electron temperatures are of the same order of magnitude as the gas temperature that was deduced from the fluid dynamic measurements (3000°K) and are too low to explain the measured degree of ionization. (Based on a typical gas density of 10^{16} cm^{-3}, an electron temperature of about 7500°K would be required to explain the 1% degree of ionization on the basis of the Saha equation; the actual electron temperature must exceed the one implied by the Saha equation by a considerable amount because of the wall and convection losses.) Thus, it is concluded that the nonlinear plasma conductivity may be a consequence of a non-Maxwellian electron-energy distribution. The high-energy tail of the distribution function may be overpopulated with energetic electrons which maintain the ionization within the moving gas stream. This conclusion is supported by the nonlinear nature of the conductivity, the double-probe measurements, and the observations concerning the effect of the inner body on the power input to the plasma. Measurement in the test section using double probes (which sample only the high-energy tail of the electron distribution) indicate electron temperatures of about 10 ev. In the discussion of the inner body experiments it was noted that although the inner body absorbed considerable energy from the plasma it did not exert a significant effect on the power input. This implies that the electron wall losses that were caused by the inner body did not influence the power transfer to the plasma —i.e., that the plasma electrical conductivity was somewhat independent of the degree of ionization, an important characteristic of a Coulomb dominated plasma.

Two final observations concerning the fluid dynamics in the large accelerator were: 1) impact pressure traverses across the test section channel indicated the presence of a mixing region when the inner body was present, and 2) in the absence of the inner body the impact pressure was uniform to within about 15% across the channel.

Most of the experiments were conducted under conditions that correspond to lines A-B in Fig. 1. A few experiments were conducted using CO_2 as a test gas since cryopumping with LN_2 baffles permitted the accelerator to be operated under conditions corresponding to quadrant II. Under these conditions the Mach number was observed to decrease along the accelerator channel as would be expected from the one-dimensional theory.

Table 3 Supersonic operating conditions

Entrance conditions	
Flow rates:	0.5–2.0 gm/sec argon
Velocity:	1675–2590 m/sec (5500–8500 fps)
Mach No.:	2.9–6.0
Temperature:	500°–2000°K
Exit conditions	
Velocity:	1950–2500 m/sec (64–8200 fps)
Mach No.:	1.45–2.2
Effective temperature:	2700°–5000°K
Density:	1×10^{-4}–5×10^{-4} kg/m^3
Static pressure	0.10–1.0 torr
Miscellaneous data	
Field velocity:	5340 m/sec
Magnetic field strength:	150–205 gauss
Total power input (accelerator):	0.25–2.5 kw
Run times:	1–5 min
Beam size:	1.5–5 in.
Exit chamber pressure:	0.085–0.5 torr

Experimental Results with 1½-in.-diam Accelerator

The primary objectives of the experiments with the small accelerator were of a fluid dynamic nature, i.e., an assessment of the extent of the end field effects and the applicability of the one-dimensional equations to the acceleration process. The design of the subsonic accelerator was a compromise between conflicting requirements, i.e., the requirement of keeping the channel diameter small enough so that a supersonic flow could be maintained with the available pumping equipment, and the requirement of providing enough ampere-turns of accelerating coil on the channel circumference so that a measurable interaction between the plasma and the traveling magnetic field would occur. As a consequence it was necessary to design the accelerator channel with an unfavorable length-to-diameter ratio. However, the channel friction was not so great as to preclude the maintenance of supersonic flow throughout the length of the channel and it is believed that some meaningful experimental observations were obtained.

The range of operating conditions for the experiments are shown in Table 3. Although some experiments were conducted with nitrogen most of the work was done with argon.

The data in the table refer exclusively to the argon experiments.

It was possible to achieve channel entrance Mach numbers of between 2.9 and 6 by using inserts to vary the throat diameter of the entrance nozzle. Measurements of the impact and static pressure in the test section during cold flow tests indicate that these Mach numbers were reduced to between 1.4 and 2.0 by the channel friction. The channel flow is shown schematically as line C-D in Fig. 1. When the traveling magnetic field was turned on and adjusted following the procedures described previously, significant increases were observed in the Mach number and luminosity at the channel exit. Impact pressure increases as high as 20% and Mach numbers as high as 2.2 were observed in the test section. The impact pressure profile in the test section exhibited a central core with a strong radial dependence. The resulting flow is indicated schematically by the line CE in Fig. 1.

Based on one-dimensional flow, the stagnation enthalpy at the entrance to the accelerator channel for a typical test was 1800 Btu/lb with 72% in kinetic energy. When the accelerator was not in operation, friction and heat transfer reduced the stagnation enthalpy at the test section to 1500 Btu/lb, with 49% in kinetic energy. Under typical operating conditions the stagnation enthalpy in the test section was increased to 2160 Btu/lb and the kinetic energy fraction to 52%.

The local variations in luminosity along the accelerator channel indicated significant end field heating at both the accelerator channel entrance and exit. Light-level measurements at the channel entrance, mid-region, and exit, made with the light-pipe photomultiplier combinations, indicated that the end field effects were greatest at the entrance.

Calorimetric measurements of the power input to the plasma stream yielded values in the range 250 w to 2.5 kw. Estimates of the average electrical conductivity obtained using Eq. (1) and neglecting the apparent axial variations in the power input gave values of between 130 and 500 mho/m. Since no probe or microwave measurements were made in these experiments, no attempt was made to relate these values to the kinetic processes within the accelerator.

Conclusions

Experiments conducted with a subsonic traveling wave accelerator in the altitude range 175,000 to 275,000 ft yielded stable plasmas that could be faithfully reproduced on a day-to-day basis. Run times of as long as $1\frac{1}{2}$ hr at power levels of over 50 kw caused no channel damage. Because of the stability of the device the conditions in the plasma exhaust stream were measured in some detail,[18] and the stream was subsequently used to test airborne electrostatic probes[19] and to perform microwave slot-antenna experiments.[20] The experimental evidence indicates that this stability is caused, at least in part, by the fact that the azimuthal currents close on themselves without passing through an electrode surface.

The experimental results imply that the plasma was dominated by Coulomb collisions and that the electron distribution function may have been non-Maxwellian. If the plasma is indeed dominated by Coulomb collisions, seeding the gas stream with a material of low-ionization potential would be expected to have little or no effect on the plasma conductivity, since the Coulomb conductivity is independent of the degree of ionization and depends only on the electron temperature.

One-dimensional analyses indicate considerable promise for the use of traveling wave accelerators in providing ultra-high velocity gas streams (15,000 to 30,000 fps) having densities in the altitude range 150,000 to 300,000 ft (the lower altitudes corresponding to the lower velocities—see Fig. 3). Facilities operating in this region would require rf power supplies in the 10- to 50-Mw range. Vacuum-tube power amplifiers of this size are within the current technology. Recent studies have indicated that radial magnetic strengths of 0.3 webers/m^2 may be possible through the use of Litz wire with appropriate cooling.[11] Preliminary studies indicate that suitable nonconducting channel walls for 50-Mw accelerators can be fabricated from commercially available materials.[5]

The experiments described in this paper were conducted with constant-field-velocity, constant-channel-area accelerators. However, the performance implied by Fig. 3 can be achieved only with accelerators in which the traveling field increases in velocity as it passes down the channel, and in which the channel has a diverging geometry as shown in Fig. 2. The channel geometry itself should offer no problem. However, in the case of the variable field velocity, coil and electrical system designs must be developed which maintain the field strength in the face of the expanding channel diameter and the increasing field velocity. Large gradients in either the field velocity or the magnetic field strength will result in excessive joule heating—an identical phenomenon to that which caused the end field heating which was observed in the supersonic experiments.

References

[1] Kerrebrock, J. L., "Segmented Electrode Losses in MHD Generated with Non Equilibrium Ionization," Rept. 178, May 1964, Avco Everett Research Lab., Everett, Mass.

[2] Meyer, R., "Magnetic Plasma Propulsion by Means of Traveling Sinusoidal Field," *Plasma Acceleration*, edited by S. W. Kash, Stanford University Press, Stanford, Calif., 1960, pp. 37–46.

[3] Smotrich, H., Janes, G. S., and Bratenahl, A., "Experimental Studies of Magnetohydrodynamic C. W. Traveling Wave Accelerator," *Proceeding of the 4th Symposium on the Engineering Aspects of Magnetohydrodynamics*, Institute of Electrical and Electronic Engineers, New York, 1963, pp. 73–92.

[4] Rocard, J. J. et al., "Development of Alternating Current Plasma Accelerator for Application as an Ultra-High Velocity Tunnel," AFFDL-TR-64-157, Nov. 1964, Air Force Flight Dynamics Lab., Wright-Patterson Air Force Base, Ohio.

[5] Thornton, J. A., Seemann, G. R., and Penfold, A. S., "Development of a Continuous Flow Electromagnetic Alternating Current Traveling Wave Accelerator for High-Density, Hypervelocity Tunnel Applications," AFFDL-TR-6745, June 1967, Air Force Flight Dynamics Lab., Wright-Patterson Air Force Base, Ohio.

[6] Williams, J. C., "Performance Similarity Between the Traveling Wave Pump and the Crossed Fields Accelerator," *ARS Journal*, Vol. 32, No. 3, March 1962, p. 427.

[7] Resler, E. L., Jr. and Sears, W. R., "The Prospects of Magneto-Aerodynamics," *Journal of the Aerospace Sciences*, Vol. 25, No. 4, April 1958, pp. 235–246.

[8] Dahlberg, E., "On the One-Dimensional Flow of a Conducting Gas in Crossed Fields," *Quarterly of Applied Mathematics*, Vol. 19, No. 3, Oct. 1961, pp. 177–193.

[9] Ring, L. E., "Optimization of MHD Crossed-Field Accelerators and Generators," paper presented at Fifth Symposium on Engineering Aspects of Magnetohydrodynamics, Massachusetts Institute of Technology, April 1–2, 1964.

[10] Ring, L. E., "Status of MHD Accelerators for Test Facilities," *Advances in Plasma Dynamics*, edited by T. P. Anderson and R. W. Springer, Northwestern University Press, Evanston, 1967, pp. 193–233.

[11] Hadelman, C., personal communication, Department of Aeronautics and Astronautics, Massachusetts Institute of Technology, Cambridge, Mass.

[12] Thornton, J. A., Seemann, G. R., and Penfold, A. S., "Experimental Study of Plasma Flow Processes in the Traveling Wave Accelerator," paper presented at 7th Symposium on Engineering Aspects of Magnetohydrodynamics, Princeton Univ., March 30, 1966.

[13] Thornton, J. A., "Abrupt Intensity Transitions in rf Generated Plasma," *Journal of Applied Physics*, Vol. 40, No. 8, July 1969, pp. 3404–3406.

[14] Knipp, C. T., "Relative Intensities of Magnetic and Electrostatic Illumination Components in the Electrostatic Discharge," *Physical Review*, Vol. 37, March 1931, pp. 756–759.

[15] Clarkson, R. E., Field, R. E., Jr., and Keefer, D. R., "Electron Temperatures in Several rf General Plasmas," *AIAA Journal*, Vol. 4, No. 3, March 1966, pp. 546–547.

[16] Seemann, G. R., Thornton, J. A., and Penfold, A. S., "Experimental Study of a Traveling Wave Accelerator," *AIAA Journal*, Vol. 4, No. 10, Oct. 1966, pp. 1870–1872.

[17] Seemann, G. R., Penfold, A. S., and Thornton, J. A., "The Minimum Specific Energy and Electric Field Necessary to Sustain a Flowing Induction Plasma," *Journal of Applied Physics*, Vol. 39, No. 1, Jan. 1968, pp. 340–342.

[18] Seemann, G. R., Thornton, J. A., and Penfold, A. S., "Subsonic Plasma Tunnel for Evaluating Re-Entry Flight Instrumentation," *AIAA Journal*, Vol. 6, No. 8, Aug. 1968, pp. 1592–1594.

[19] Seemann, G. R. and Thornton, J. A., "Experimental Investigation of a Flush Electrostatic Double Probe for Re-Entry Measurements," AIAA Paper 69-700, San Francisco, Calif., 1969.

[20] Warder, R. C., Jr. and Thornton, J. A., "An Experimental Study of the Breakdown Characteristics of Microwave and VHF Antennas, Vol. 1," AFCRL-68-0450, July 1968, Air Force Cambridge Research Lab., Cambridge, Mass.

JUNE 1970 AIAA JOURNAL VOL. 8, NO. 6

Effect of Mass Injection on a High-Current Arc

RODNEY L. BURTON,* PIERRE DEVILLERS,† AND ORSON CHANG†
University of California, San Diego, La Jolla, Calif.

To understand better the MPD arc and other accelerating high-current arcs, experimental and theoretical investigations are presented for a parallel-plate quasi-steady arc with argon or helium injection from a linear slit at the midplane. The arc is quasi-steady for about 350 μsec, and the quasi-steady current is 4–14 ka. Mass flow rate is set and controlled by an electromagnetically driven gas valve. It is found that at low mass flow rate the arc inductance oscillates, but that at a sufficiently high mass flow rate $\dot{m}_c$, the arc voltage becomes constant. Measurements of $\dot{m}_c$ in argon and helium show a dependence $\dot{m}_c \sim I^2/u_c$, where $u_c = (2eV_i/m)^{1/2}$ is the critical speed corresponding to the ionization potential. In addition, arc voltage is found to increase linearly with current. A simplified theoretical model is developed, based on one-dimensional constant area flow of a monofluid. Two physical constraints must be imposed to determine the downstream flow conditions, and these are 1) sonic downstream flow, and 2) $\dot{m}$ adjusts to minimize arc power input. These constraints predict $\dot{m} \sim I^2/u_c$, and an electrical impedance $Z \sim u_c$. Both of these results show reasonable agreement with experiment. Application of the theory to high-current arcs with no mass injection indicates that the electrodes erode at a rate proportional to I^2.

I. Introduction

ONE of the most intriguing questions to be asked about accelerating arc discharges is that of how the arc utilizes the mass flow available to it. An early and most celebrated fact about the MPD arc was its ability to produce thrust with no input mass flow,[1] due to the utilization of background mass and/or electrode material. It has also been observed[2–5] that the arc parameters of thrust and voltage are independent of the mass flow rate over a wide range. This behavior suggests that the MPD arc in some manner adjusts the amount of mass to be accelerated, independently of the mass fed into it, and mechanisms for this adjustment have been proposed by Cann,[6] Bennett et al.,[3] and Stratton.[7]

In this paper some experiments on quasi-steady parallel-plate arcs will be described, and the results will be compared with previous theory and with a one-dimensional arc model.

Presented as Paper 69–266 at the AIAA 7th Electric Propulsion Conference, Williamsburg, Va., March 3–5, 1969; submitted July 22, 1969; revision received December 29, 1969. This research was supported by the Advanced Research Projects Agency of the Department of Defense and was monitored by the U. S. Army Research Office-Durham under Contract DA-31-124-ARO-D-257. The authors are indebted to W. A. Conner for the construction of the apparatus, and to J. C. Sherman for his critical comments on the paper.

* Assistant Professor of Engineering Physics, Department of Aerospace and Mechanical Engineering Sciences. Member AIAA.

† Graduate Student, Department of Aerospace and Mechanical Engineering Sciences.

II. Previous Experiments

In previously reported work[8] it was demonstrated that an arc current of up to 50 ka in a parallel-plate accelerator could be stabilized by partially insulating the electrodes. This result has also been achieved by Eckbreth and Jahn.[9] The arc chamber, shown in Fig. 1, is rectangular with internal dimensions 10 × 10 × 25 cm. The chamber is filled with argon at a pressure of 0.075–0.60 torr, and the electrodes are driven by a 35 μsec flat-topped pulse of current, of 25–50 ka. With magnetic probe coils (Fig. 1), it was demonstrated that after a short transient phase, the magnetic field pattern becomes nearly steady. In addition, the voltages V_0 and V_{28} are equal in steady operation (Fig. 1), so that the magnetic flux threading the electrodes between the probes is a constant. Since the magnetic pressure behind the sheet at 50 ka is 1.4 atm, the fluid is pumped in the positive x direction.

It was clear from the results that this arc, operating with no mass injection, primarily accelerates electrode material. Severe pitting occurs in the brass electrodes, although not in the nylon insulator, and electrode material is plated onto the downstream endwall. It is calculated that the argon fill available to the arc is depleted during the time of the discharge, assuming that the argon is fully ionized and that the argon energy is on the order of the ionization potential. This view is also supported by Kerr Cell photographs of the discharge, showing that the plasma is only luminous near the electrodes.

For future comparison with the mass-injected arc, which does not run on electrode material, it will be useful to summarize the results of terminal and internal measurements for the case of no mass injection; 1) arc voltage is independent